Ref. Ares(2022)1675923 - 07/03/2022

High-Performance Advanced Methods and Experimental Investigations for the Safety Evaluation of Generic Small Modular Reactors

Research and Innovation Actions

Horizon 2020, Topic NFRP-2019-2020-05:
Support for Safety Research of Small Modular Reactors

2020 – Research and Innovation Framework Programme

Contract Number: 945063
Start Date: 01/09/2020 Duration: 36 Months

This project has received funding from the Euratom research and training programme 20019-2020 under grant agreement No 945063.

– Deliverable –

D3.7: Transient decay heat model for Serpent

Summary

One of the main objectives of the McSAFER project is to estimate the added benefit of using beyond the state-of-the-art high-fidelity methods for reactor core physics compared to state-of-the-art reduced order methods. This will be achieved by modeling the same small modular reactor (SMR) transients using high fidelity and reduced order methods.

Serpent 2 continuous energy Monte Carlo particle transport code within the Kraken framework constitutes part of the two steps Serpent-Ants calculation chain that aims to provide full core reduced-order neutronics solution via Ants nodal diffusion solver based on the pre-calculated (micro-group constants) data from Serpent, as well as high-fidelity, reference, solution by itself.

The availability of an advanced thermal energy deposition model in the time-dependent calculations to be conducted in the project is a must to produce accurate power distributions in transient or accident scenarios and design-basis parameters definition.

A group-based decay heat curve-fitting methodology is proposed within the future needs of Serpent calculations simulations to be conducted in Task 3.4 of the McSAFER project.

Proprietary Rights Statement

This document contains information which is proprietary to the McSAFER Consortium. Neither this document nor the information contained herein shall be used, duplicated or communicated by any means or any third party, in whole or in parts, except with the prior consent of the McSAFER Consortium.

Disclaimer

The content of this document reflects only the authors' views and the European Commission is not responsible for any use that may be made of the information it contains.

McSAFER – Contract Number: 945063
High-Performance Advanced Methods and Experimental Investigations for the Safety Evaluation of Generic Small Modular Reactors.

Document Information

Document title	**Transient decay heat model for Serpent**
Author(s)	**Ana Jambrina, Ville Valtavirta**
Number of pages	23
Document type	Deliverable
Work Package	WP3
Document number	D3.7
Issued by	VTT
Date of completion	25/02/2022
Dissemination level	Public

Document History

Rev.	Date	Comments & status	Author
0	25/02/2022	First complete draft	Ana Jambrina
1	25/02/2022	Final draft	Ana Jambrina

Document Approval

Rev.	Main author(s)	Verification	Approval
Name	Ana Jambrina	Ville Valtavirta	Victor Sanchez
Date	07/03/2022	07/03/2022	07/03/2022
Signatures			

Distribution List

Name	Organisation	Comments
Panagiotis MANOLATOS	EC DG RTD	

Partner n°	Beneficiary short name	Type of beneficiary	Country
1	KIT	University and research centre	Germany
2	LUT	University	Finland
3	CEA	Research centre	France
4	UJV	Private company	Czech Republic
5	HZDR	Research centre	Germany
6	JACOBS	Private company	England
7	VTT	Research centre	Finland
8	JRC	European Research Centre	EU
9	PEL	Utility	Germany
10	UPM	University	Spain
11	TRACTEBEL	Private company	Belgium
12	KTH	University	Sweden
13	CNEA	Research Centre	Argentina

Distribution to the partners will be through the project SharePoint.

Table of contents

1. Introduction

Serpent 2 continuous energy Monte Carlo particle transport code [1] within the Kraken framework [2] constitutes part of the two steps Serpent-Ants calculation chain that aims to provide full core reduced-order neutronics solution via Ants nodal diffusion solver [3] based on the pre-calculated (micro-group constants) data from Serpent, as well as high-fidelity, reference, solution by itself.

In this study, Serpent will be applied as a state-of-the-art high fidelity neutronics solver to provide detailed level results for the NuScale SMR core transients in WPs 3 and 5 of the McSAFER project.

For such simulations, an advanced thermal energy deposition model in time-dependent calculations is a must to produce accurate power distributions in transient or accident scenarios and design-basis parameters definition.

2. Thermal energy deposition models in nuclear reactors: background

2.1. Energy deposition rates: overview

The total energy released by a fission event has several prompt and delayed energy contributors [4]. Although, primarily, the recoverable energy is released instantaneously as kinetic energy from fission products and fission neutrons, prompt gamma rays or energy, from the subsequent neutron capture. Only a part of it is emitted after as, radioactive decay of fission products and radioactive nuclei due to neutron capture as delayed beta and gamma rays. After a period of steady power history, of the order of magnitude of days, its equilibrium is reached. Consequently, its time dependence is no longer represented in reactor core solvers aside from the decay heat production during reactor shutdown or post-accident scenarios. Some transient scenarios, i.e., a slow transient due to core depletion and a fast transient, such as a reactivity-initiated accident (RIA), might question such simplification.

2.2. Decay heat model: overview

The decay heat is the thermal energy released through the radioactive decay of fission products and nuclides produced by the neutron capture in fission products and actinides produced by the neutron capture in heavy metals. It constitutes the second-largest source of thermal power within the reactor, and thus, it should be accurately modelled at any time of the reactor operation. It plays an important role, not only in the analysis of transient/accident scenarios, e.g., loss of coolant, main steam line break, etc., but also as a safety design parameter, e.g., spent fuel storage, final disposal sites, etc.

Table 1: Energy deposition contributors [4]

a)	Fission a) Kinetic energy of Fission Products b) Prompt and Decay Beta Particle Energy

b)	Neutron Capture a) Kinetic Energy of Charged Particles b) Decay Beta Particle Energy c) Nuclear Recoil
c)	Neutron Scattering a) Nuclear Recoil Following Elastic Scattering Interactions b) Nuclear Recoil Following Inelastic Scattering and Subsequent Nuclear De-Excitation
d)	Photon Sources a) Prompt Fission b) Fission Product Decay c) Neutron Capture d) Inelastic Scatter De-Excitation e) Transmutation Product Decay f) Positron Annihilation g) Bremsstrahlung h) Atomic De-Excitation
e)	Photon Transport
f)	Photon Interactions a) Photoelectric Absorption b) Compton Scattering c) Pair Production d) Photonuclear Reactions

From Table 1 can be foreseen the complexity of evaluating the heat production in nuclear reactors, due to the multiple inherent parts that constitute the phenomenon. Mainly, the following four groups: a) fission heat released, b) heat released from neutron capture, scattering, etc., c) heat released from the decay of fission products, d) heat released from the decay of activation products. Table 2 shows a quantitative example of the different components of the heat released after a fission event.

Table 2: Quantitative example of the different components of the heat released after a fission event

Daughter nuclei	169.13 MeV
Prompt neutrons	4.838 MeV
Delayed neutrons	0.0074 MeV
Prompt gammas	6.6 MeV
Delayed gammas	6.33 MeV
Delayed betas	6.5 MeV
Neutrinos	8.75 MeV
Total	202.16 MeV
Total minus neutrinos	193.4 MeV

2.3. Time-dependent thermal energy deposition modeling: overview

The traditional evaluation of the thermal power [5] either in steady-state or time-dependent calculations accepts equilibrium delayed power, forsaking the time-dependence of the decay power from the precursors.

The power at time t due to the energy released from neutron fission and capture rates, and is normalized to produce the true thermal power of the reactor,

$$P(t) = F(t)\sum_j V_j\left(\sum_i q_{f,i}N_i(t)\sum_g \sigma_{f,g,i,j}\phi_{g,j}(t) + \sum_i q_{c,i}N_{i,j}(t)\sum_g \sigma_{c,g,i,j}\phi_{g,j}(t)\right) \quad (1)$$

where:

$F(t)$	flux normalization factor
$q_{f,i}$	direct fission energy release for isotope i
$q_{c,i}$	recoverable energy per neutron capture for isotope i
V_j	volume of material region j
$N_{i,j}$	number density of isotope i in material region j
$\phi_{g,j}$	neutron flux of energy group g in region j
$\sigma_{f,g,i,j}$	microscopic fission cross section
$\sigma_{c,g,i,j}$	$\sigma_{a,g,i,j} - \sigma_{f,g,i,j}$, microscopic capture cross section
$\sigma_{a,g,i,j}$	microscopic absorption cross section
$P(t)$	thermal power of the reactor

** Approximately 7% of the total recoverable fission energy constitutes the delayed term.

The general formulation of the reactor thermal power, $P(t)$, can be written as the sum of a prompt component $P_p(t)$, and a delayed component $P_d(t)$.

$$P(t) = P_p(t) + P_d(t) \quad (2)$$

For an isotope, iso, the fraction γ_i^f and γ_i^c correspond, respectively, to the fission and capture energy release some time after the fission or capture event. This way, the prompt thermal power, $P_p(t)$, can be written as,

$$P_p(t) = F(t)\sum_j V_j\sum_i\sum_{x=f,c}(1-\gamma_i^x)q_{x,i}N_{i,j}(t)\times\sum_g \sigma_{x,g,i,j}\phi_{g,j}(t) \quad (3)$$

To determine the delayed thermal power, $P_d(t)$, two main approaches can be followed. A general approach is to lump the numerous components of the delayed heat source into a relatively small number of "groups" (*group-based* methodology). On the other hand, a rigorous calculation based on a detailed fuel inventory for each time step, where each contributor is explicitly represented (*explicit* methodology), tracks independently all the nuclides involved within the calculation. The fidelity and the computational cost and memory demand are proportional.

Following the *group-based* methodology is described as it is the most common approach within (reduced order) neutronics solvers, and its extension to the explicit representation does not involve major changes besides the number of independent nuclides or "groups".

The *group-based* approach is similar to the treatment of delayed neutron precursors. The characterization of each "group" is based on the half-lives of the delayed heat groups. Defining $C^x_{m,i,j}$ as the concentration of the delayed heat group m of isotope i at region j for the induced reaction x and, being the balance equation that $D^x_{m,i,j}$ satisfies given by,

$$\frac{dC^x_{m,i,j}(t)}{dt} = F(t)V_j\gamma^x_{m,i}q_{x,i}N_i(t)\sum_g \sigma_{x,g,i,j}\phi_{g,j}(g) - \lambda^x_{m,i}C^x_{m,i,j}(t) \quad (4)$$

where $\gamma^x_{m,i}$ and $\lambda^x_{m,i}$ are the yield and decay constants of the delayed heat group m. Thus, $\sum_m \gamma^x_{m,i}$ represents γ^x_i in Eq. ((*3*). Giving $C^x_{m,i,j}$, the delayed power is defined as,

$$P_d(t) = \sum_j \sum_i \sum_{x=f,c} \sum_m \lambda^x_{m,i}\, C^x_{m,i,j}(t) \quad (5)$$

Eq. (1) should be substituted by Eqs. (2)-**Error! Reference source not found.** to solve for the time dependence of delayed energy. Let's note that Eq. **Error! Reference source not found.** has the same form as the delayed neutron precursor equation. The analytical solution, assuming a constant delayed heat source $S^x_{m,i,j} = FV_j\gamma^x_{m,i,}q_{x,i}N_{i,j}\sum_g \sigma_{x,g,i,j}\phi_{g,j}$ within a standard burnup time step or sub-step (t_1, t_2), results into,

$$C^x_{m,i,j}(t) = C^x_{m,i,j}(t_1)\exp\left(-\lambda^x_{m,i}(t-t_1)\right) + \frac{S^x_{m,i,j}}{\lambda^x_{m,i}}\left[1-\exp\left(-\lambda^x_{m,i}(t-t_1)\right)\right], \qquad t_1 \le t \le t_2 \quad (6)$$

The predictor-corrector time integrator relaxes the previously assumed hypothesis referred to the delayed heat source $S^x_{m,i,j}$.

The definition of the average $C^x_{m,i,j}$ over a time step Δt used for the flux normalization is given as,

$$\bar{C}^x_{m,i,j} = \frac{1}{\Delta t{\lambda^x_{m,i}}^2}\left(\left[S^x_{m,i,j} - \lambda^x_{m,i}C^x_{m,i,j}(t_1)\right]\exp\left(-\lambda^w_{m,i}\Delta t\right) + \lambda^x_{m,i}C^x_{m,i,j}(t_1) + \lambda^x_{m,i}S^x_{m,i,j}\Delta t - S^x_{m,i,j}\right) \quad (7)$$

Consequently, the flux normalization factor is described as,

$$F(t) = \frac{P(t) - \sum_j \sum_i \sum_{x=f,c} \sum_m \lambda^x_{m,i}\bar{C}^x_{m,i,j}}{\sum_j V_j \sum_i \sum_{x=f,c}\left(1-\gamma^x_i\right)q_{x,i}N_{i,j}(t)\sum_g \sigma_{x,g,i,j}\phi_{g,j}(t)} \quad (8)$$

The coupled system defined by Eq. (*8*) and Eq. (4) is iterated to solve for $F(t)$ and $C^x_{m,i,j}(t)$. The converged normalization factor F is used within the depletion calculation in the current step.

The methodology considers two approximations: (i) Eq. (*6*) assumes that the delayed energy source $S^x_{m,i,j}$ is a constant within a time step under the framework of a predictor-corrector depletion calculation; (ii) Eq. (*8*) uses a time-averaged $\bar{C}^x_{m,i,j}$ to estimate the average delayed power over a time step.

The normalization factor F is derived from the steady-state calculation, being constant throughout the transient. However, at each time-step, the thermal power is updated. Eqs. (2)-(6) model the delayed power explicitly, leading to a constant $S^x_{m,i,j}$ within the time-step. Finally, the flux at the end of the time step is used to compute the new $S^x_{m,i,j}$.

3. Serpent 2: current status, challenges and limitations

3.1. Heat deposition modeling: current status (steady-state)

The most traditional way in which Serpent models heat production and deposition is based on the very simple concept of computing all components as one: 202.27 MeV deposited per single fission event of ^{235}U, covering all heating, prompt and delayed (note that fissions of other nuclides compute other values).

Depletion calculations have a more accurate evaluation of decay heat based on the nuclide specific activity and the energy release per single decay.

Recently, new models for advanced heat deposition methods [6] for neutron and photon reactions have been included in Serpent 2. However, delayed gamma and beta components that follow the changes in fission rate with a delay are not accurately accounted for.

3.2. Time-dependent challenges and limitations

In general terms, there are three key points to consider when evaluating transients and heat deposition modeling: a) the computational cost burden associated with Monte Carlo time-dependent calculations, b) the significance of the time-dependence of the heat release, and c) the multi-component aspect of the heat deposition. Those components are the following: a) prompt energy release by fissions and other neutrons (and photon reactions), b) energy released from the decay of nuclides existing at the start of the transient, and c) energy release from radioactive nuclides produced during the transient.

Figure 1 show some transient heat release scenarios from which some challenges and limitations for each of the current (and previously mentioned) heat deposition modeling are foreseen: a) the single-component approach has no time-dependence: limited physical background, b) depletion calculations require tracking hundreds or thousands of nuclides and evaluating transmutations cross sections, with the computation cost associated: potentially suited for evaluating "*Decay of pre-existing*", and c) the advanced heat deposition models for neutron and photon reactions: well suited for evaluating "*Prompt energy release*". Therefore, there would be still a missing component: "*Decay*

of newly created". Nonetheless, it is aimed to develop a general and common approach to handle both decay components, "*pre-existing*" and "*newly created*".

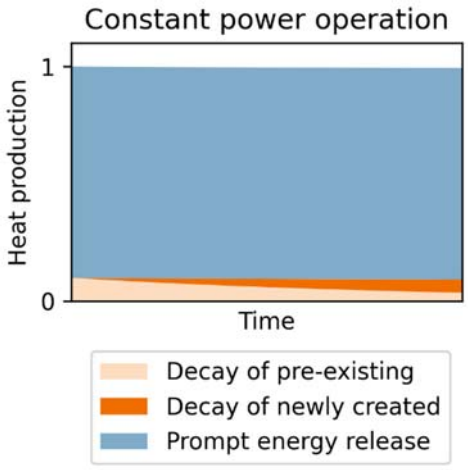

1) Transient heat release in a simulation of constant power operation transient (Simplified model).

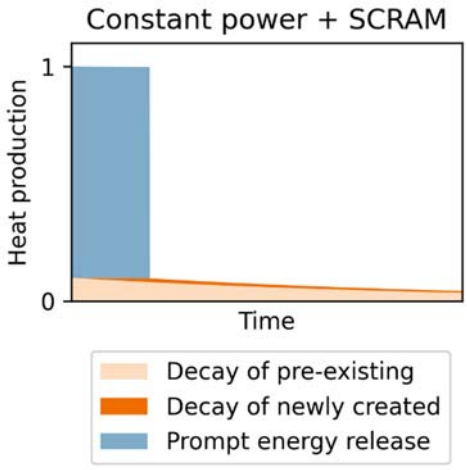

2) Transient heat release in a simulation of constant power operation followed of SCRAM transient (Simplified model).

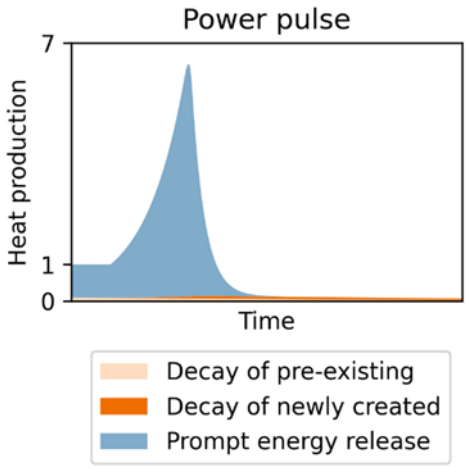

3a) Transient heat release in a simulation of a power pulse, RIA scenario, transient (Simplified model)

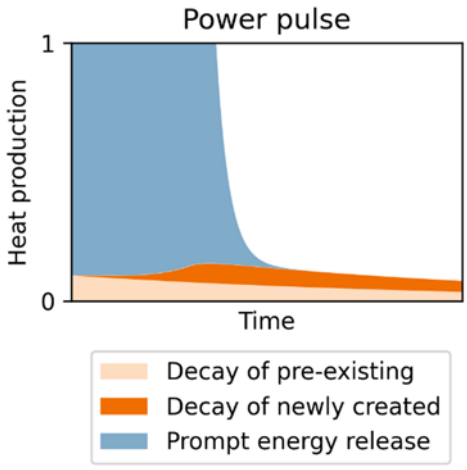

3b) Transient release in a simulation of a power pulse, RIA scenario, transient (Detailed model)

Figure 1: Transient heat release scenarios

4. Potential approaches for decay heat evaluation for Serpent 2

Next, three potential approaches are outlined, giving a brief overview of the methodology and highlighting the major anticipated challenges of the modeling and implementation.

- Approach 1: explicit depletion
- Approach 2: transient analog material compositions
- Approach 3: group-based decay heat fitting

4.1. Approach 1: explicit depletion

The *explicit* methodology for delayed energy thermal deposition allows an accurate prediction of the decay heat evolution for any reactor system, e.g., thermal and fast, and fuel type, without the imposed assumptions, e.g., derived from the semi-empirical correlations defined over a limited range of burnup and fuel types characterizing the *group-based* methodology.

This approach is based on an explicit evaluation of the transmutation reaction rates followed by the solution of the coupled non-linear depletion system.

Serpent accounts for the spatial nuclide composition at a local operational history during burnup, at the end of each time step Δt, by solving the full set of Bateman equations, Eq.(*9*). It computes the matrix exponential using a built-in depletion solver based on the Chebyshev Rational Approximation Method, CRAM [7] (for $\mathbf{N} = [N_j]$ the local (j-region) nuclide composition vector and, $\mathbf{A}$ the transmutation matrix, including neutron-induced and decay reactions).

$$\mathbf{N}(t + \Delta t) = \exp(\mathbf{A}\Delta t)\mathbf{N}(t) \quad (9)$$

The number of tracked nuclides and transmutation chains derive from the nuclear data, and it is subject of adjustments via Serpent input. By evaluating the contribution of the full set of nuclides during all depletion and decay steps, Serpent allows an explicit calculation of the local (j-region) nuclide decay heat $\mathbf{P}_{dh} = [P_{dh,j}]$ as,

$$\mathbf{P}_{dh}(t) = \sum_i \mathbf{N}_i(t)\lambda_i q_i \quad (10)$$

where:

$\mathbf{P}_{dh}(t)$	local decay heat rate vector at time t
$\mathbf{N}_i(t)$	local isotope i concentration vector at time t
λ_i	decay constant for isotope i
q_i	energy release per decay for isotope i

The decay constants and the energy released per decay for each nuclide are obtained from the radioactive decay data file based on a given nuclear data evaluation. Serpent calculates the local fuel nuclide compositions on the run using the actual local fluxes and the pre-calculated microscopic cross sections, dependent on the local operational parameters.

Besides of the computational burden derived from the depletion calculation, a clear challenge arises from the fact that Serpent tracks nuclides in time-dependent calculations in a continuous manner, while, by definition, burnup calculations would represent fixed time-intervals.

4.2. Approach 2: transient analog material compositions

The *transient analog* approach could be considered a mid-point between the *explicit* methodology and the *group-based* methodology. It is based on knowledge of the initial compositions and the evolution over time-intervals pre-calculated radioactive decay dependent compositions, decay heat release and delayed photon emission.

During the time-dependent calculation, removal of neutron absorbing nuclides and addition of reaction production(s) are evaluated in an analog manner, with the associated difficulties in getting a proper sampling.

The main challenges inferred from this approach lie in the fact that the changes in material compositions over time due to decay would affect the cross sections, with the implication of recalculating majorants, etc. Furthermore, the non-negligible assumption of constant material composition during the time interval should be made to track the nuclides in the given interval. The computational cost would be increased due to not only involve simply decay single nuclides, but also the whole chain decay.

4.3. Approach 3: group-based decay heat

The *group-based* methodology is inspired by the delayed neutron group precursors approach, and widely implemented in deterministic solvers, where instead of tracking concentrations of hundreds or thousands of exponentially decaying individual nuclides, concentrations of (10-20) decay “groups” are tracked.

The constants for the *group-based* delayed heat data, analogously to the associated data to the delayed neutron precursors, can be obtained by fitting the energy release as a function the emission time. The delayed heat data can be derived from, e.g., the ANS-5.1 decay heat standard for LWRs [8], which provides either tabular data at discrete cooling times or exponential fit of the tabular data.

The standard relies on the direct fission of four fissile isotopes (^{235}U, ^{238}U, ^{239}Pu, ^{241}Pu). There is no independent data from the neutron capture absorber, only for the overall fission products. In such scenario, it could be assumed the capture energy is prompt, i.e., $\gamma_i^c = 0$.

$$P_{dh}(t) = \sum_{m=1}^{M=23} \alpha_m \exp(-\lambda_m t) \quad (11)$$

Eq. (*11*) represents the decay heat power at t seconds after a fission pulse from a fissionable isotope. The solution of integrating Eq. (*11*) over time is the total delayed heat release after a fission pulse.

$$E_{dh} = \int_0^{\infty} P_{dh}(t)dt = \sum_{m=1}^{M=23} \frac{\alpha_m}{\lambda_m} \quad (12)$$

Based on the previously described delayed heat model and the total direct fission energy release for fissionable isotope q_m, the delayed yield γ_m is defined as,

$\gamma_m = \frac{\alpha_m}{\lambda_m q_m}$	(13)

Other standards, such DIN Norm 25463 [9] or *group-based* curve-fitting methodologies, e.g. Dunn's approach [10], implemented in reactor core simulators, produce similar overall decay heat estimate depending on the assumption consider in the formulation.

The most direct challenge associated with the *group-based* methodology lies on the nature of data, meaning, how good that limited, general and predefined data fits into a high-fidelity Monte Carlo calculation.

5. Generic derivation of a decay heat group-based model

Alternatively of using the ANS-5.1 standard 23 group-wise exponential parameters, a "best" group structure fitting methodology is presented based on the Levenberg-Marquardt optimization algorithm [11] for the problem-dependent data pre-calculated from Serpent, and the underlying ENDF neutron-induced fission yields and decay data.

The methodology is described in two stages:

- Before transient:
  The initial material compositions are transformed into the so-called "decay heat groups" by fitting the decay heat from the initial compositions into the group structure. The first step allows modeling the so-called "*Decay of pre-existing*".
  The fitting is based on the actual decay heat solution from Serpent for the full depletion system, and the accuracy of the given fitting is user-defined.

- During transient:
  The decay of the group-wise concentrations is calculated during the time intervals, and the group concentrations are modified/added based on fission (and activation rates). The second step allows modeling the so-called "*Decay of newly created*".
  The production of decay heat concentrations from fission (and activation) reactions has to be otherwise solved.

Note: from now on, all results shown in this report are calculated with Python (KrakenTools) based on micro-depletion, fission yield, decay, and reaction data from Serpent.

5.1. Fitting a "best" group structure to a decay heat curve

The Levenberg-Marquardt optimization algorithm [12] solves a non-linear least squares curve fitting problem, which in this context means the minimization of the sum of the squares of the differences

between the decay heat function pre-calculated by Serpent and the multi-exponential fit being optimized.

The formulation of the optimization problem is

$$F(\boldsymbol{p}) = \sum \left(f(t) - \hat{f}(t,\boldsymbol{p})\right)^2 = \left(\boldsymbol{f} - \hat{\boldsymbol{f}}(\boldsymbol{p})\right)\left(\boldsymbol{f} - \boldsymbol{f}(\boldsymbol{p})\right)^T \quad (14)$$

where the goal is to find the set of parameters $\boldsymbol{p}$ minimizing the cost function. The local minimum will be reached when, via an iterative process, a given perturbation $\boldsymbol{\delta}$ no longer contributes to reduging the cost function.

The algorithm combines two non-linear least-squares methods: Gauss-Newton and gradient descendent. The Gauss-Newton method locally approximates the least-squares function as a quadratic function and solves for the minimum of this function. The gradient descent method calculates the steepest-descend, updating the parameters searching for a smaller sum of squared errors.

The gradient descendent method calculates the direction of the steepest descendent starting from the current parameter values, by evaluating the gradient of the cost function with respect to the parameters and taking a step in the opposite direction. The gradient can be written as follows

$$\frac{\partial}{\partial \boldsymbol{p}} F(\boldsymbol{p}) = 2\left(\frac{\partial}{\partial \boldsymbol{p}}\left(\boldsymbol{f} - \hat{\boldsymbol{f}}(\boldsymbol{p})\right)\right)\left(\boldsymbol{f} - \hat{\boldsymbol{f}}(\boldsymbol{p})\right)^T = -2\frac{\partial \hat{\boldsymbol{f}}(\boldsymbol{p})}{\partial \boldsymbol{p}}\left(\boldsymbol{f} - \hat{\boldsymbol{f}}(\boldsymbol{p})\right)^T \quad (15)$$

where $J = \partial \hat{\boldsymbol{f}}(\boldsymbol{p})^T / \partial \hat{\boldsymbol{f}}(\boldsymbol{p})$ is the Jacobian, and therefore, the perturbation $\boldsymbol{\delta} = \boldsymbol{\alpha} J\left(\boldsymbol{f} - \boldsymbol{f}(\boldsymbol{p})\right)^T$ being α a positive value.

The Gauss-Newton method search for a quadratic function with respect to the parameters in the vicinity of the optimal solution. This assumption holds for smooth functions. Any errors derived from the given assumption will be corrected through the iterative convergence process.

The function, approximated by a first-order expansion, is written as

$$\hat{\boldsymbol{f}}(\boldsymbol{p}+\boldsymbol{\delta}) \approx \hat{\boldsymbol{f}}(\boldsymbol{p}) + \frac{\boldsymbol{\partial \hat{f}}(\boldsymbol{p})}{\partial \boldsymbol{p}}\boldsymbol{\delta} \approx \hat{\boldsymbol{f}}(\boldsymbol{p}) + J^{\boldsymbol{T}}\,\boldsymbol{\delta} \quad (16)$$

Now, the gradient of the cost function with respect to the perturbed step is given by

$$\frac{\partial}{\partial \boldsymbol{p}} F(\boldsymbol{p}+\boldsymbol{\delta}) \approx -2\,J\left(\boldsymbol{f} - \hat{\boldsymbol{f}}(\boldsymbol{p})\right)^T + 2\,J\,J^{\boldsymbol{T}}\,\boldsymbol{\delta} \quad (17)$$

Solving for an unbounded perturbation**,** meaning $\partial F(\boldsymbol{p}+\boldsymbol{\delta})/\partial \boldsymbol{p} = 0$, then $\boldsymbol{\delta} = \frac{\mathbf{1}}{J\,J^{\boldsymbol{T}}} J\left(\boldsymbol{f} - \hat{\boldsymbol{f}}(\boldsymbol{p})\right)^T$.

Given the similarities between the optimal step produced by the Gauss-Newton and gradient descendent methods, Levenberg proposed a combination of both methods by using the step defined as

$$\boldsymbol{\delta} = \left(\frac{\mathbf{1}}{J\,J^{\boldsymbol{T}}} + \, dI\right) J\left(\boldsymbol{f} \, - \, \hat{\boldsymbol{f}}(\boldsymbol{p})\right)^{T} \rightarrow \boldsymbol{\delta} = \left(\frac{\mathbf{1}}{J\,J^{\boldsymbol{T}}} + \, d\; diag\left(J\,J^{\boldsymbol{T}}\right)\right) J\left(\boldsymbol{f} \, - \, \hat{\boldsymbol{f}}(\boldsymbol{p})\right)^{T} \quad (18)$$

where d represents a damping parameter [13].

Notes: small values of d compared to the elements in $J\,J^{\boldsymbol{T}}$ correspond to the Gauss-Newton method, while large values shift the algorithm towards the gradient descendent method

The second representation, replacing the identity matrix by the diagonal elements of $J\,J^{\boldsymbol{T}}$ infers normalization of the damping parameter d with respect to each of the elements of diagonal.

The iterative process searches a minimization of the cost function $F(\boldsymbol{p})$ for a given step $\boldsymbol{\delta}(\boldsymbol{p})$ where the stopping criteria [14] for each new step $\boldsymbol{\delta}$ is calculated as

$$\rho = \frac{F(\boldsymbol{p}) \; - F(\boldsymbol{p} + \boldsymbol{\delta})}{\boldsymbol{\delta}^{T}\left(d\; diag(J\,J^{\boldsymbol{T}})\;\boldsymbol{\delta} + J\left(\boldsymbol{f} \, - \, \hat{\boldsymbol{f}}(\boldsymbol{p})\right)^{T}\right)} \quad (19)$$

where the numerator represents the difference in the cost function given by the step $\boldsymbol{\delta}$ and the denominator is Taylor's expansion approximation of the cost function.

The iterative scheme is described as follows:

- $\rho > 0$: implies a reduction of the cost function $F(\boldsymbol{p})$.
  a) if $\rho > \epsilon$ (threshold) the step is accepted. Simultaneously, decreasing the damping parameter d will bring it closer to the Gauss-Newton method, which shows good performance in the vicinity of the optimal $\boldsymbol{p}*$.
  b) if $\rho < \epsilon$ can be discarded and recomputed with a larger damping parameter d which will bring it closer to the gradient descendent method (and decrease the step size)

- $\rho < 0$: indicates an increase in the cost function $F(\boldsymbol{p})$ and therefore, the step is rejected.

The proposed iterative algorithm is defined with the following performance criteria, for $\epsilon = 10^{-4}$

- if $\rho > \epsilon$
  - $\boldsymbol{p} \leftarrow \boldsymbol{p} + \boldsymbol{\delta}$
  - $d \leftarrow max\left[{}^{d}/_{2}, 10^{-7}\right]$
- else
  - $d \leftarrow min[2d, 10^{7}]$

when the step is accepted the parameters $\boldsymbol{p}$ are updated and the Jacobian and the cost function are recalculated accordingly.

The curve-fitting iterative algorithm requires a starting point for the calculations, aka an initial guess for the fit. From Eq. (*11*), each exponential function requires two parameters: α and λ.

Note:

At the beginning of the decay heat calculation ($t = 0$), the sum of the exponential functions of the form $\hat{f}(t) = \alpha\ exp(-\lambda t)$ is described by the sum of α's (group-wise yields). The initial guesses for the α's are formed by equidistant points (number of exponential functions, e.g., $n = 23$) starting from the total decay heat at $t = 0$ and ending with the smallest contributor to the decay heat which are normalized by the total decay heat at $t = 0$. → $[\alpha_1, \dots,\ \alpha_n] = \left[sum\left(P_{dh,i}, \dots, min\left(P_{dh,i}\right)\right)\right]$

The initial guesses for the λ's (group-wise half-lives) are described by equidistant points too, starting from the decay constant that a single exponential would have to correspond with the decay heat function provided by Serpent at the end points of the curve fitting and ending with the largest decay constant included in the calculation. → $[\lambda_1, \dots,\ \lambda_n] = \left[\frac{1}{-T} ln\left(\frac{P(T)}{sum\left(P_{dh,i}\right)}\right), \dots, max(\lambda_i)\right]$

5.2. Ensuring positivity of decay constants and concentrations

The previous proposed curve-fitting methodology does not limit the α's (group-wise yields) and λ's (group-wise half-lives) to positive values keeping a physical meaning.

For such a purpose the exponential function can be redefined as follows:

$\hat{f}(t) = \alpha\ exp(-\lambda t)$	$\hat{f}(t) = \alpha^2\ exp(-\lambda t)$	$\hat{f}(t) = \alpha^2\ exp(-\lambda^2 t)$	(20)

which, consequently, have an impact in the definition of the Jacobians.

5.3. Targeting minimum of absolute or relative difference

The cost function $F(\boldsymbol{p})$, originally described by the absolute difference between the trial fit and the target function can be represented instead by the relative difference, to balance the difference and the actual value.

$F(\boldsymbol{p}) = \left(\boldsymbol{f}\ -\ \hat{\boldsymbol{f}}\,(\boldsymbol{p})\right)\left(\boldsymbol{f}\ -\ \boldsymbol{f}\,(\boldsymbol{p})\right)^T$	$F(\boldsymbol{p}) = \left(\frac{\boldsymbol{f}}{\hat{\boldsymbol{f}}\,(\boldsymbol{p})} - 1\right)\left(\frac{\boldsymbol{f}}{\hat{\boldsymbol{f}}\,(\boldsymbol{p})} - 1\right)^T$	(21)

which, consequently, have an impact in the definition of the Jacobians.

5.4. Converting existing material compositions to group concentrations.

The transformation of the initial material composition to decay heat groups takes place by fitting the decay heat from initial compositions into the group structure. The fit is based on the actual decay heat solution from Serpent for the full depletion system.

The fitting corresponds with the α's of the known group structures, for pre-defined λ's (fixed, ANS standard-based) to find the "fixed" set of α's for the given group-structure or the "best" set of α's and λ's when both parameters are targets of the fitting.

Figure *2* shows the difference between a "fixed" fitting vs a "best" fitting in terms of the decay heat curve representation and the absolute and relative error between the target and the trial functions. Clearly a "tailored" approach results in a better fitting option $R^2 = 0.95 \rightarrow R^2 = 1.0$.

Figure *3* outputs the difference between the "fixed" and "best" values of the λ's for the given group structure.

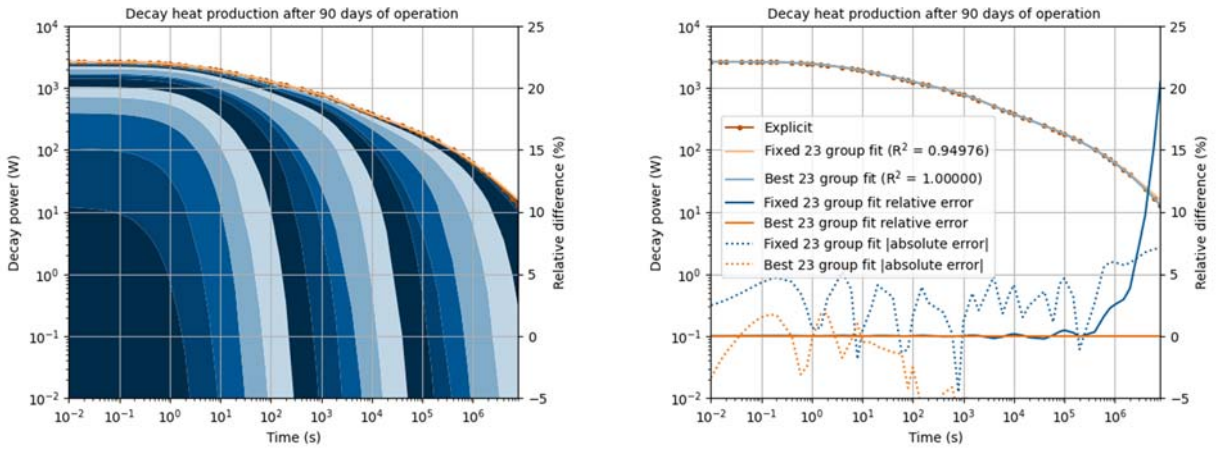

Figure 2: Decay heat production after 90 days of operation (LWR assembly)

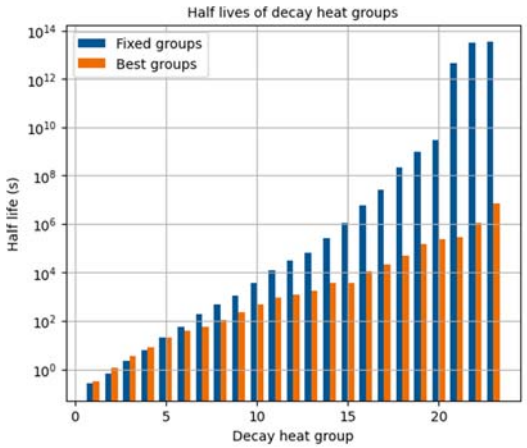

Figure 3: Half-lives of the 23 decay heat groups „*Decay of pre-existing*"

5.5. Converting fission yields to group yields.

The contribution to each group yield, which will define the evolution of the group concentrations during the transient due to fission, is evaluated by fitting the α's of the known group structure to the decay heat curve obtained from the depletion of fission yield distribution.

Figure *4* and Figure *5* represent, respectively, such contribution to the decay heat groups and the associated half-lives for a fitting with $R^2 = 0.95$.

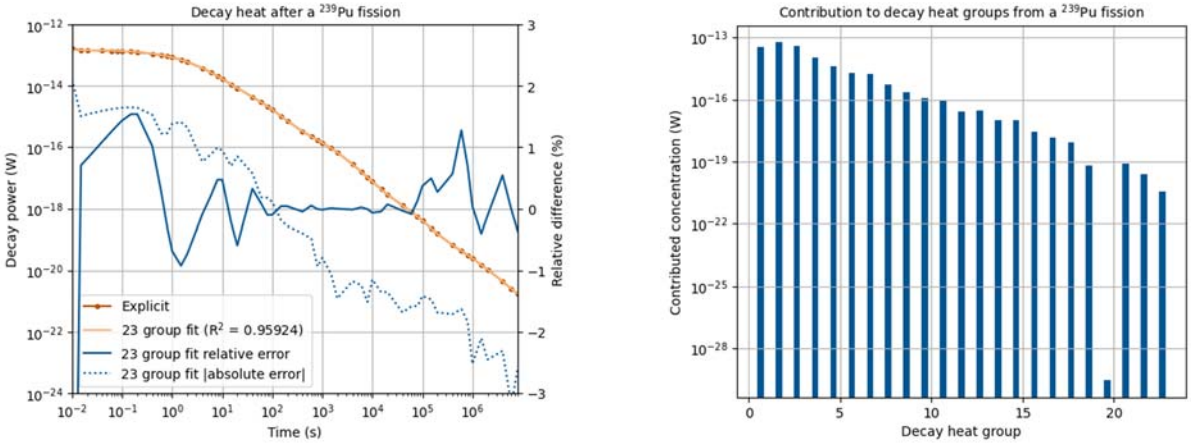

Figure 4: Decay heat after a ^{239}Pu fission pulse and contribution to the decay heat groups

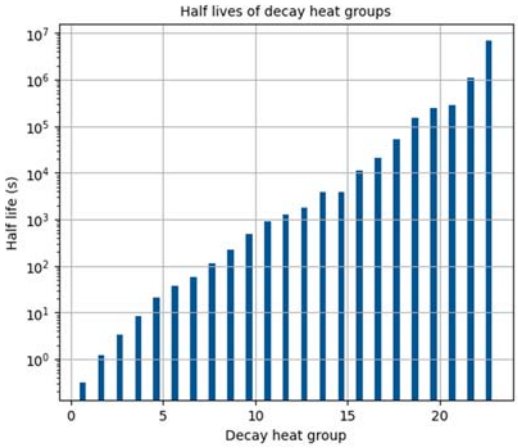

Figure 5: Half-lives of the 23 decay heat groups „*Decay of newly created*“

5.6. Convergence studies for fitting

A semi-realistic test case is based on a Serpent calculation with dozen(s) of material zone divisions described by a PWR-like fuel assembly: McSAFER-NuScale C02 assembly with burnable absorbers. The depletion history sequence goes up to 40 MWd/kgU to evaluate the fitting at different burnup state points, e.g., 0, 5, 20 and 40 MWd/kgU.

Highlights:

- The adaptation of the damping parameter and how the fitting methodology is shifted towards the Gauss-Newton method or the gradient descendent method in each iteration and whether to accept a proposed step seems to be the most important iterative decision

- The initial guess might have a significant effect at the beginning of the fitting process that might be corrected with an appropriated convergence criteria via threshold(s) and damping parameters. However, finding a reasonable guess defines the course of the iteration. E.g., by coarsely gridding the parameter space or random search on the objective function finding a combination that results in a minimum value.

Both, the adaptation of the damping parameter and the initial guess are the two main contributors to the convergence process. Other factors are:

- Imposing $\alpha > 0$ and $\lambda > 0$, and therefore redefining the exponential functions seems to not have a significant effect on the iteration process, fading away with other elements.
- Representing the cost function via relative/absolute difference has a larger impact for states where the absolute values are rather small.

Other aspects to consider would be the time-scale and the group structures (including the number of groups), fuel-type, etc.

5.7. Limitations and open questions

The proposed *group-based* methodology for decay heat curve-fitting modelling is still under development and some open question and potential limitations have to be studied in detail. Some of them are listed above,

- The geometrical entity carrying out the tracking of the concentration lies in mapping the depleted material zone divisions in correspondence with a generic mesh or detector bin structure. This underlying bottleneck is a known issue in Serpent.
- While the current approach accounts for decay heat released by activation products (including actinides) that are present in the beginning of the transient, any new activation products that are created during the transient simulation are not included in the decay heat evaluation. The implications of this simplification will require further studies; it is uncertain the contribution of those activation products newly created during the transient is in any way significant for the decay heat evaluation.
- Conversely, the group formalism does not account for radioactive nuclide removal due to neutron reactions during the transient, only production from fission reactions.
- This methodology, analogously to the advanced energy deposition methods recently implemented in Serpent does not account for the delayed gamma and beta emission components that follow the changes in fission rate with a delay.
- The *group-based* approach analyzed through KrakenTools seems to be robust and well suited to be implemented in Serpent. However, a more realistic case scenario and the whole Monte Carlo transient system will require further analysis of the methodology to ensure its readiness.

6. Required implementations in Serpent 2

To outline the current (Serpent 2.1.32) and the proposed transient calculation scheme, Table 3 and Table 4, respectively, present in a nutshell the different steps that constitute the transient simulation.

With a brief description of each stage, it is aimed to provide a flavor of the requirements of the proposed decay heat model implementation in Serpent 2.

Table 3: Current transient calculation scheme, Serpent 2.1.32

(Step 1)	Source generation: neutron transport criticality calculation
(Step 2)	Transient external source simulation with constant decay heat

Table 4: Proposed transient calculation scheme

(Step 0)	Depletion of the whole model at the given initial burnup state point of the transient
(Step 1)	Source generation: neutron transport criticality calculation ▪ Generation of initial data for the fitting and transient simulation: 1. Material compositions 2. Mapping: material compositions vs. mesh-based/detector-based 3. ENDF data: neutron-induced fission yields and decay data
(Step 2)	"Predictive" depletion/decay calculation ▪ Decay heat curve generation: 1. Global system decay heat curve (seconds to minutes) → Used for fitting lambdas 2. Decay heat curves for each material (seconds to minutes) → Used for converting the initial material nuclide concentrations to initial material group concentrations. 3. Decay heat curves for each fission yield distribution (seconds to minutes) → Used for producing group fission yield distributions
(Step 3)	Fitting ▪ Proposed methodology
(Step 4)	Transient simulation ▪ <u>At the beginning of each time interval:</u> Calculate decay of group concentrations for each material 1. Evaluation of energy release 2. Update of end of time-interval concentrations

	▪ <u>During neutron tracking:</u> Calculate the production of decay heat precursors 1. Analog/implicit evaluation of the decay heat precursors following delayed neutron precursors approach 2. Based on the fission group yields, estimation of the group production per single interaction. Part of which will decay before the end of the time-interval, released as heat, and the remaining part will be added to the decay concentrations. ** The remaining question is how to score the energy release at the different stages.
(Step 5)	New (restart) independent calculation

7. Summary

A method was needed for evaluating decay heat in Serpent 2 continuous energy Monte Carlo transport particle code in order to produce accurate power distributions in transient or accident scenarios and design-basis parameter definitions.

After considering various options the so-called *group-based* approach was chosen as the first step in upgrading the energy deposition modeling in time-dependent calculations for its simplicity in the implementation, the ability to stage the transient calculation, and, overall, not adding computational burden to an already costly simulation.

The process of fitting generic group structures was described and its applicability to this problem was demonstrated with KrakenTool using Serpent-based data.

The required modifications to the normal Serpent transient calculation scheme were described and the implementation of the methodology in Serpent will take place during the remaining period of the McSAFER project.

References

[1] J. Leppänen, M. Pusa, T. Viitanen and V. Valtavirta, "The Serpent Monte Carlo code: status, development and applications in 2013," *Annals of Nuclear Energy,* vol. 82, pp. 142-150, 2015.

[2] J. Leppänen, V. Valtavirta, A. Rintala, V. Hovi, R. Tuominen, J. Peltonen, M. Hirvensalo, E. Dorval and U. Lauranto, "Current Status and On-Going Development of VTT's Kraken Core Physics Computational Framework," *Energies,* vol. 15, no. 3, p. 876, 2022.

[3] V. Salhberg and A. Rintala, "Development and first results of a new rectangular nodal diffusion solver of Ants," in *PHYSOR 2018*, 2018.

[4] ANSI/ANS-19.3.4-2002(R2017), "The Determination of Thermal Energy Deposition Rates in Nuclear Reactors," American Nuclear Society Standards, 2017.

[5] Y. Liu, B. Kochunas and W. Martin, "Delayed fission energy effect on LWR normal operation and transients," *Annals of Nuclear Energy,* vol. 128, pp. 84-93, 2019.

[6] R. Tuominen and V. Valtavirta, "New energy deposition treatment in the Serpent 2 Monte Carlo transport code," *Annals of Nuclear Energy,* vol. 129, pp. 224-232, 2019.

[7] M. Pusa, "High-order Chebyshev rational approximation method and application to burnup equations," *Nuclear Science and Engineering,* vol. 182, pp. 297-318, 2016.

[8] ANSI/ANS-5.1-2014(R2019), "Decay Heat Power in Light Water Reactors," American Nuclear Society Standards, 2019.

[9] DIN Norm-25463, "Berechnung der Nachzerfallsleistung der Kernbrennstoffe von Leichtwasserreaktoren," Deutsches Institut für Normung, 1990.

[10] F. E. Dunn, "Decay Heat Calculations for Transient Analysis," *Transactions of the American Nuclear Society,* vol. 60, pp. 633-634, 1989.

[11] T. Kalinainen, "Modelling of Decay Heat with Exponential Functions in Serpent 2," Aalto University, 2016.

[12] D. W. Marquardt, "An Algorithm for Least-Squares Estimation of Nonlinear Parameters," *Journal of the Society for Industrual and Applied Mathematics,* vol. 11, no. 2, pp. 431-441, 1963.

[13] H. B. Nielsen, "Damping parameter in Marquardt's method," Technical University of Denmark, 1999.

[14] H. P. Garvin, "The Levenberg-Marquardt method for nonlinear least squares curve-fitting problems," Duke University, 2016.